Contents lists available at ScienceDirect

European Journal of Pharmacology

journal homepage: www.elsevier.com/locate/ejphar

Molecular and Cellular Pharmacology

Tailoring elastase inhibition with synthetic peptides

Andreia Vasconcelos [a], Nuno G. Azoia [a], Ana C. Carvalho [b], Andreia C. Gomes [b], Georg Güebitz [c], Artur Cavaco-Paulo [a,*]

[a] Universidade do Minho, Departamento de Engenharia Têxtil, Campus de Azurém, 4800-058, Guimarães, Portugal
[b] Centre of Molecular and Environmental Biology (CBMA), Department of Biology, Campus de Gualtar, 4710-057, Braga, Portugal
[c] Department of Environmental Biotechnology, Graz University of Technology, A-8010 Graz, Austria

ARTICLE INFO

Article history:
Received 10 January 2011
Received in revised form 13 May 2011
Accepted 22 May 2011
Available online 2 June 2011

Keywords:
Human neutrophil elastase (HNE)
Inhibition kinetic
Bowman–Birk inhibitor
Peptide
Wound exudate

ABSTRACT

Chronic wounds are the result of excessive amounts of tissue destructive proteases such as human neutrophil elastase (HNE). The high levels of this enzyme found on those types of wounds inactivate the endogenous inhibitor barrier thus, the search for new HNE inhibitors is required.
This work presents two new HNE inhibitor peptides, which were synthesized based on the reactive-site loop of the Bowman–Birk inhibitor protein. The results obtained indicated that these new peptides are competitive inhibitors for HNE and, the inhibitory activity can be modulated by modifications introduced at the N- and C-terminal of the peptides. Furthermore, these peptides were also able to inhibit elastase from a human wound exudate while showing no cytotoxicity against human skin fibroblasts in vitro, greatly supporting their potential application in chronic wound treatment.

1. Introduction

Human neutrophil elastase (HNE) (EC 3.4.21.37) is a serine protease of the chymotrypsin family that is stored in the primary (azurophil) granules of polymorphonuclear neutrophils (PMNs) and is released by inflammatory stimuli. Under normal conditions the activity of HNE is regulated by endogenous inhibitors like secretory leukocyte protease inhibitor and elafin. The continuous activation of inflammatory cells is followed by the release of large quantities of HNE which inactivate the inhibitor defense. Excessive and uncontrolled HNE activity has been implicated in mediating tissue damage associated with chronic wounds and other major chronic inflammatory diseases including rheumatoid arthritis (Ekerot and Ohlsson, 1984) and chronic obstructive pulmonary disease (Shapiro, 2002). In the area of wound healing, the presence of high levels of HNE is associated with the degradation of important growth factors (Yager et al., 1997) and major proteins of the extracellular matrix like fibronectin (Grinnell and Zhu, 1994) which are vital for the normal wound healing process. Due to its involvement in such pathological processes, there has been considerable interest in the design of HNE inhibitors that may restore the normal levels of this enzyme in the above diseases. Apart from natural or engineered inhibitor proteins of high molecular mass, there has been an increasing interest in studying both peptide-based and non-peptide small inhibitor compounds (Edwards and Bernstein, 1994).

The Bowman–Birk inhibitors are bi-headed serine proteinase inhibitors found in plants of the Fabaceae family (Norioka and Ikenaka, 1983). These proteins have a low molecular weight (6–9 kDa) and are characterized by the presence of seven disulphide bridges which allow the formation of a symmetrical structure comprising two independent heads located at opposite sides of the molecule (see Fig. 1). Each head is made of a tricyclic domain in which the functional reactive site loop is located. Loop I typically inhibits trypsin and loop I' inhibits chymotrypsin (Chen et al., 1992; Lin et al., 1993; Voss et al., 1996; Werner and Wemmer, 1992). The interaction of Bowman–Birk inhibitor with serine proteases occurs via a well-defined disulfide linked short beta-sheet region which generates a non-covalent complex that renders the serine protease inactive (McBride and Leatherbarrow, 2001). The conformation of the reactive site loop is complementary to the active site of the protease inhibited and allows Bowman–Birk inhibitor to tightly bind to the protease (Chen et al., 1992). Bowman–Birk inhibitor-derived synthetic peptides have previously been demonstrated to retain the inhibitory activity of the complete protein (McBride et al., 2002).

The present work is based on the ability to retain inhibitory activity of short peptide sequences that reproduce the reactive site-loop of Bowman–Birk inhibitor protein (Mcbride et al., 1999; Nishino et al., 1977; Odani and Ikenaka, 1973; Terada et al., 1978). The synthetic peptide sequences were tested as inhibitors of HNE and porcine pancreatic elastase (PPE) to determine the specificity of the peptides. Furthermore, the inhibitory activity of these peptides was

* Corresponding author. Tel.: +351 253510100; fax: +351 253510293.
E-mail address: artur@det.uminho.pt (A. Cavaco-Paulo).

0014-2999/$ – see front matter © 2011 Elsevier B.V. All rights reserved.
doi:10.1016/j.ejphar.2011.05.056

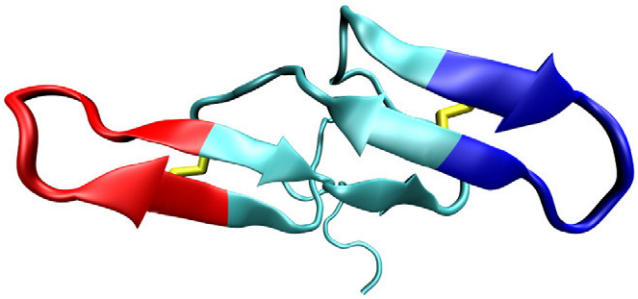

Fig. 1. Three-dimensional structure of soybean trypsin/chymotrypsin Bowman–Birk inhibitor in solution (PDB code 1BBI (Werner and Wemmer, 1992)). Loop I as shown is red, loop I' is blue and the disulphide bond is yellow.

also tested using chronic wound exudate, in order to evaluate their ability to be used as a part of a wound management strategy.

2. Materials and methods

The Porcine Pancreatic Elastase (PPE), Human Neutrophil Elastase (HNE) and Elastatinal were purchase from Sigma, Spain. The peptides 2 (MGWCTASVPPQCYG, 1499.75 g/mol) and 3 (MGWCTASVPPQCYG $(GA)_7$, 2339.62 g/mol) were synthesized by JPT Peptide Technologies GmbH (Germany). The BJ5ta cell line (telomerase-immortalized human normal skin fibroblasts) was purchased from the European Collection of Cell Cultures (ECACC) and cultured according to ATCC recommendations. All other reagents, including those used in cell culture, were analytical grade and purchased from Sigma, Spain.

2.1. Collection of wound exudate

Wound exudate was collected from pressure wounds using a vacuum assisted closure system by the Medisch Spectrum in Twente. Wound fluid samples were weighed and 100 µl of phosphate buffer pH 7.0 were then added to 10 mg of wound fluid. Samples were incubated at room temperature for 1 h and then centrifuged at 1000 *g* for 20 min to remove cells and tissue-material. After centrifugation the wound exudate was sterilized using Oxy Fil Centrifugal Filter (0.2 µm membrane pore diameter). The samples were then ready for storage at −20 °C until further use. The total protein content in the wound exudate was determined by the Lowry method (Lowry et al., 1951).

2.2. Determination of activity loss over time

The half-life times for HNE, exudate and PPE were determined following the incubation with different concentrations of inhibitor peptides (20–80 µM) at 25 °C. The concentrations of HNE, exudate and PPE were 20 µg/ml, 2.4 µg/ml and 175 µg/ml respectively. At determined time points, aliquots were taken and the activity was determined against the synthetic substrates, 5 mM of N-Methoxysuccinyl-Ala-Ala-Pro-Val-p-nitroanilide for HNE and exudate. A stock solution of this substrate of 20 mM was prepared in DMSO (dimethyl sulfoxide). To prepare the 5 mM solution, the required amount of the stock solution was added to 0.1 M HEPES buffer, 0.5 M NaCl, pH 7.5. The substrate used for PPE was N-Succinyl-Ala-Ala-Ala-*p*-nitroanilide, 4.4 mM prepared in 0.1 M Tris–HCl buffer, pH 8.0. The absorbance was monitored for 5 min at 410 nm using a Heλios γ ThermoSpectronic spectrophotometer. Control assays were performed in the same conditions but without inhibitor. Measurements were recorded in triplicate and the results were expressed as mean value ± S.D. (standard deviation).

2.3. Inhibition kinetics

The inhibition kinetics of the peptides was determined by competitive binding studies (Domingo et al., 1995; Gariani et al., 1999). Briefly, 15 µl of proteases (HNE (20 µg/ml)), exudate (2.4 µg/ml) and PPE (175 µg/ml) were incubated with 15 µl of peptide inhibitors (20–80 µM) for 30 min at 25 °C. The final volume of each sample was adjusted to 300 µl with 0.1 M HEPES buffer, 0.5 M NaCl, pH 7.5 (HNE and exudate) and 0.1 M Tris–HCl buffer, pH 8.0 (PPE). The reaction was initiated with the addition of an adequate volume of substrate to obtain a substrate concentration range of 100–3000 µM. The substrate for HNE and exudate is N-Methoxysuccinyl-Ala-Ala-Pro-Val-p-nitroanilide 5 mM and for PPE is N-Succinyl-Ala-Ala-Ala-*p*-nitroanilide 4.4 mM prepared in the respective buffer solutions. The residual activity was determined by the increase in the optical density at 410 nm over 10 min using a microplate reader (Varian). Control assays were performed in the same conditions without inhibitor peptides. All assays were done in triplicate and the results are expressed as the mean value ± S.D. K_i was determined by nonlinear regression analysis (Leatherbarrow, 1990) using the GraphPad Prism software (GraphPad, 2010).

2.4. Determination of IC_{50} for proteases using synthetic substrates

To determine the IC_{50} values of the inhibitor peptides against proteases, 15 µl of proteases (HNE (20 µg/ml)), exudate (2.4 µg/ml) and PPE (175 µg/ml) were incubated with 15 µl of peptide inhibitors (20–80 µM) for 30 min at 25 °C. The volume was adjusted to 300 µl with respective buffer solutions. The reaction was started after the addition of 27 µl of 400 µM of N-Methoxysuccinyl-Ala-Ala-Pro-Val-p-nitroanilide (HNE and exudate) and N-Succinyl-Ala-Ala-Ala-*p*-nitroanilide (PPE). The increase in optical density at 410 nm was monitored over 10 min using a microplate reader (Varian). All assays were done in triplicate and the results are expressed as mean value ± S.D. IC_{50} was determined using the GraphPad Prism software (GraphPad, 2010).

2.5. Determination of IC_{50} for HNE and exudate using insoluble elastin

The ability of the synthetic peptides to inhibit the hydrolysis of insoluble elastin by HNE was determined spectrophotometrically using elastin congo-red as a substrate according to the method previously described (Naughton and Sanger, 1961). Briefly, elastin congo-red (2 mg/ml) and HNE (20 µg/ml) and exudate (2.4 µg/ml) were incubated with various concentrations of peptides (20–80 µM) in 1.5 ml of 0.1 M Tris–HCl buffer, pH 8.0 containing 0.2 M NaCl at 30 °C for 1 h. After incubation, the reaction was stopped by the addition of 1.5 ml of 0.1 M acetic acid and, the mixture was centrifuged at 1500 *g* for 10 min at room temperature. After centrifugation, the absorbance of the supernatant was measured at 495 nm using a Heλios γ ThermoSpectronic spectrophotometer. Triplicate measurements were made for each inhibitor concentration and the results are expressed as mean value ± S.D.

2.6. Silk fibroin films preparation and peptide incorporation

Silk fibroin (fibroin) films were prepared as described before (Vasconcelos et al., 2010). Briefly, fibroin solution 1% (w/v) was prepared by dissolving degummed silk fibers into a saturated solution of LiBr at 60 °C for 3 h. The solution was then filtered, and dialyzed against distilled water using, cellulose tubing (molecular-weight cut-off of 12000–14000 Da), until complete removal of salts.

The peptides (40 µM) were mixed with the fibroin solution for 5 min at room temperature. After this time, solutions were cast in 24-well plates and dried overnight at room temperature. In order to induce the transition of fibroin from random coil to β-sheet structure

and consequently insolubility, the films were immersed in 90% (v/v) methanol solution for 30 min and then washed in distilled water and air dried. Films were incubated with HNE for 1 h at 25 °C and then aliquots were taken for the evaluation of HNE activity decrease as described above.

2.7. Cytotoxicity evaluation

The peptides were tested for cytotoxicity according to the ISO standards (10993–5, 2009). The BJ5ta cell line (normal human skin fibroblasts) was maintained according to ATCC recommendations (4 parts Dulbecco's Modified Eagle's Medium (DMEM) containing 4 mM L-glutamine, 4.5 g/l glucose, 1.5 g/l sodium bicarbonate, and 1 part of Medium 199, supplemented with 10% (v/v) of fetal bovine serum (FBS), 1% (v/v) of Penicillin/Streptomycin solution and 10 μg/ml hygromycin B). The cells were maintained at 37 °C in a humidified atmosphere of 5% CO_2. Culture medium was refreshed every 2 to 3 days.

Cells were seeded at a density of 10×10^3 cells/100 μl/well on 96-well tissue culture polystyrene (TCPS) plates (TPP, Switzerland) the day before experiments and then exposed to different peptide concentrations added to fresh culture medium. At 24 and 48 h of exposure, cell viability was determined using the MTS assay (CellTiter 96® Non-Radioactive Cell Proliferation Assay, Promega, EUA).

MTS tetrazolium compound (3-(4,5-dimethylthiazol-2-yl)-5-(3-carboxymethoxyphenyl)-2-(4-sulfophenyl)-2H-tetrazolium) is a colored formazan substrate which is converted by several mitochondrial and cytoplasmic enzymes in viable cells into a soluble, pink fluorescent product. 20 μl of MTS compound were added to each well containing 100 μl of culture medium. After 4 h of incubation at 37 °C the absorbance at 490 nm was measured in a microplate reader (Spectramax 340PC). The quantity of formazan formed is directly proportional to the number of viable cells. Data are presented as average ± S.D. Non-parametric, Wilcoxon matched samples test was used, with statistically significant differences when $P<0.05$. All calculations were performed using GraphPad software (GraphPad, 2010).

3. Results

In this study synthetic peptides based on the anti-trypic loop of the Bowman–Birk inhibitor protein were used for the design of new inhibitor peptides. The peptide was selected from the combinatorial library (Mcbride et al., 1999) of Bowman–Birk inhibitor-derived peptides. To the selected peptide (WCTASVPPQCYG, Fig. 2, white circles), modifications were made in the N-terminal, by the introduction of methionine (M) and glycine (G) (Peptide 2, MGWCTASVPPQCYG, Fig. 2, light gray circles). This sequence was maintained and a glycine/alanine (GA) tail (n = 7) was added to the C-terminal (Peptide 3, MGWCTASVPPQCYG(GA)7, Fig. 2, dark gray circles).

3.1. Determination of activity loss over time

The time of incubation necessary to obtain a decrease in 50% of elastase activity, was determined by incubating the peptides with PPE, HNE and wound exudate and the decrease in activity was monitored over the time as described in experimental section. In our study, it was also used elastatinal, a low molecular weight elastase inhibitor, as a control. Fig. 3, represents the activity loss obtained with the lowest concentration of peptides used (20 μM) after 30 min of incubation. It can be observed that after 30 min it was obtained more than 50% of activity loss for all the peptides. Nevertheless, both peptide 3 ($MGWCTASVPPQCYG(GA)_7$) and elastatinal present higher activity loss than peptide 2 (MGWCTASVPPQCYG), especially for HNE, indicating the higher inhibitory activity. The time of incubation determined (30 min) will be used in the further experiments.

3.2. Inhibition kinetics

In order to establish the inhibition mechanism, PPE, HNE and wound exudate were incubated with different peptide concentrations. To analyse the inhibition, Lineweaver–Burk plots, i.e. double-reciprocal plot for the hydrolysis of the synthetic substrates were determined for all the peptides and enzyme (Data not show for PPE and wound exudate). Fig. 4 represents the progress curves for the inhibition of HNE by both peptides (Fig. 4A and B) and the correspondent Lineweaver–Burk plot (Fig. 4C and D). From the analysis of the last, it can be determined the mechanism of inhibition and from the results, peptide MGWCTASVPPQCYG and $MGWCTASVPPQCYG(GA)_7$ are competitive inhibitors for HNE, PPE and wound exudate. Then, non-linear regression was applied to determine the Michaelis–Menten constant (K_m) and V_{max} by Eq. 1:

$$V = V_{max} \times \frac{[S]}{[S] + K_m} \quad (1)$$

V is the enzyme reaction velocity; V_{max} is the maximum enzyme reaction velocity which is attained when all the subsites of the enzyme are occupied by the substrate; [S] is the substrate concentration and K_m is the Michaelis–Menten constant that represents the substrate concentration when half of the binding sites are occupied. The results also confirmed the type of inhibition present because V_{max} remains

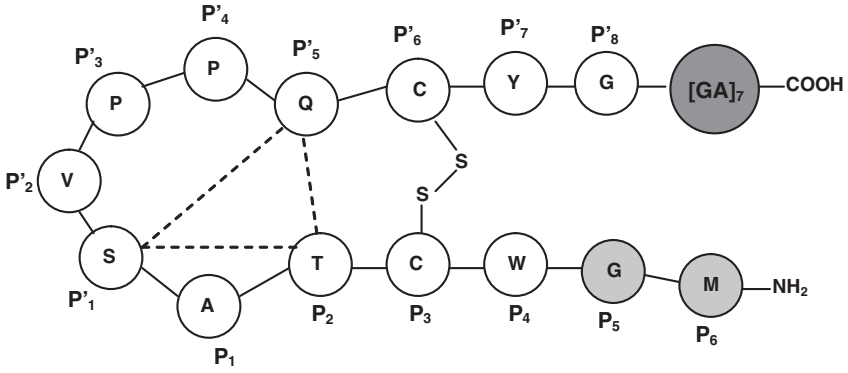

Fig. 2. Representation of the peptide sequences mimicking the reactive site loop of the Bowman–Birk inhibitor protein.

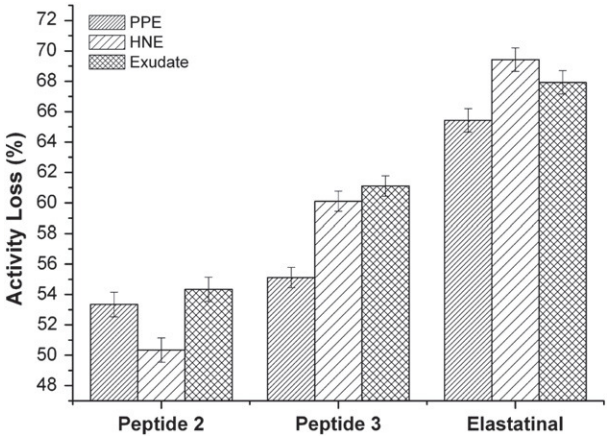

Fig. 3. Activity loss obtained after 30 min of incubation at 25 °C of elastases with 20 μM of peptides 2, 3 or elastatinal. (Peptide 2 = MGWCTASVPPQCYG, peptide 3 = MGWCTASVPPQCYG$(GA)_7$).

unchanged in the presence of different peptide concentrations and, there is an increase in the K_m. These values are higher for HNE in the presence of peptide MGWCTASVPPQCYG$(GA)_7$, indicating that this peptide causes higher inhibition. The competitive inhibition exhibited for peptides MGWCTASVPPQCYG and MGWCTASVPPQCYG$(GA)_7$ may work through direct competition with the substrate by binding to the active site, or binding to a remote site and causing a conformational change in the enzyme.

Competitive inhibitors cause an apparent increases of K_m (i.e., the inhibitor interferes with substrate binding) without affecting V_{max} (inhibitor cannot bind to the complex enzyme-substrate). Therefore, inhibition constants (K_i) were determined by the modified Michaelis–Menten equation for competitive inhibition (Eq. (2)):

$$V = V_{max} \times \frac{[S]}{[S] + K_m\left(1 + \frac{[I]}{K_i}\right)} \quad (2)$$

[I] is the inhibitor concentration and K_i (inhibition constant) is the dissociation constant of the enzyme-inhibitor complex.

The inhibition constants (K_i) obtained for the peptides are presented in Table 1. It can be observed that the inhibition constants obtained for peptide MGWCTASVPPQCYG$(GA)_7$ presents the best results, especially for HNE. There is an improvement in K_i for HNE obtained for peptide WCTASVPPQCYG (McBride et al., 2002), when amino acid residues were added to both N- and C-terminals.

The K_i ratio presented shows the selectivity of the peptides for HNE. The results indicate that peptide MGWCTASVPPQCYG$(GA)_7$ presents higher specificity for HNE. Moreover, K_i values obtained for PPE, HNE and wound exudate with the peptides are comparable, and in some cases better (MGWCTASVPPQCYG$(GA)_7$ for HNE), with the K_i obtained for elastatinal. A very important result and approach of this study, is the use of a human wound exudate. The peptides MGWCTASVPPQCYG and MGWCTASVPPQCYG$(GA)_7$ present good inhibition constants and the differences obtained when compared with HNE (Sigma) might be related with the presence of other proteases present in the exudate that can interfere with the inhibition. The hydrolytic stability of Bowman–Birk inhibitor peptides used in this study was determined by mass spectrometry analysis (Data not shown). The hydrolysis of the peptides occurred after 6 h of incubation with the studied enzymes.

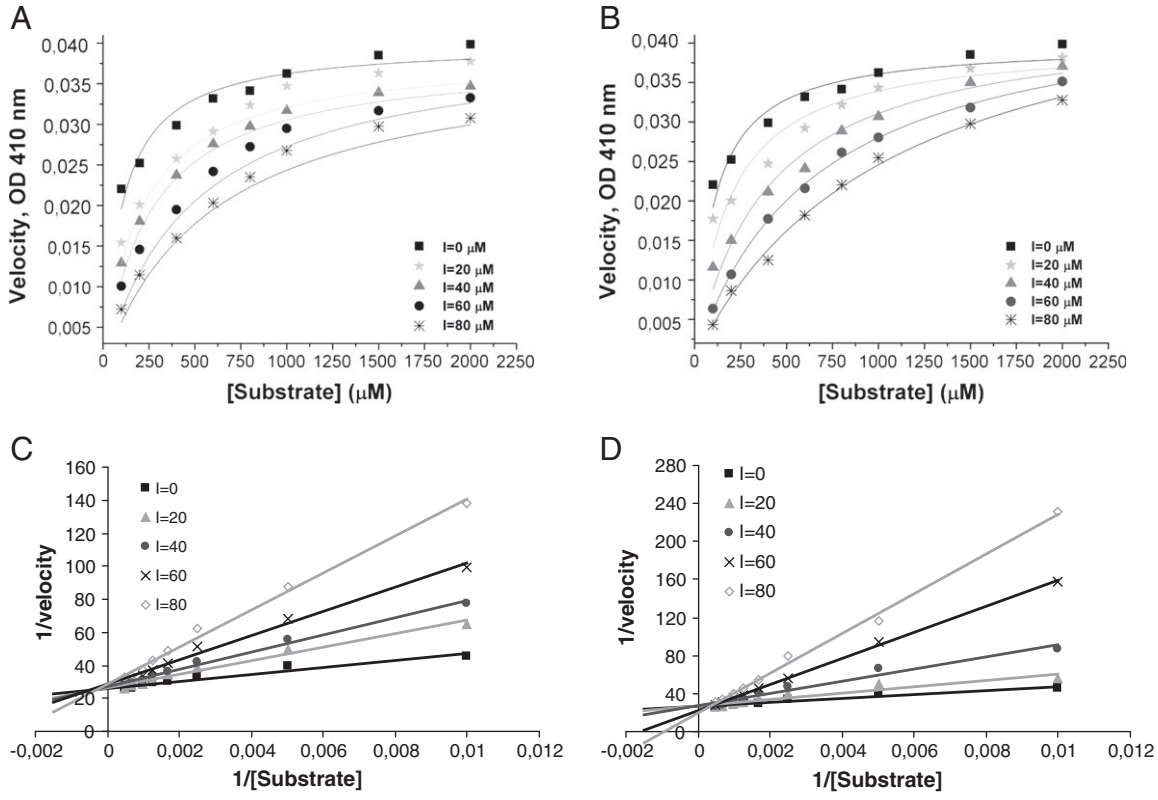

Fig. 4. Progress curves for the inhibition of HNE by peptide 2 (A) and peptide 3 (B) for the hydrolysis of the synthetic substrate. The correspondent Lineweaver–Burk plots are represented in (C) peptide 2 and (D) peptide 3. (Peptide 2 = MGWCTASVPPQCYG, peptide 3 = MGWCTASVPPQCYG$(GA)_7$).

Table 1
Inhibition constants (K_i) obtained for the peptides against PPE, HNE and wound exudate. Peptide 1 = WCTASVPPQCYG, peptide 2 = MGWCTASVPPQCYG, peptide 3 = MGWCTASVPPQCYG$(GA)_7$).

Peptide	Ki (μM)			K_iPPE/K_iHNE
	PPE	HNE	Exudate	
Peptide 1*	13	2.77	–	–
Peptide 2	8.1 ± 1.6	6.3 ± 1.2	7.0 ± 1.8	1.3
Peptide 3	7.0 ± 2.0	0.4 ± 0.01	3.1 ± 0.9	17.5
Elastatinal	9.7 ± 1.4	6.7 ± 1.1	7.8 ± 1.2	1.2

* Values were obtained from the literature (McBride et al., 2002).

3.3. Determination of IC_{50} for proteases

IC_{50} is defined as the concentration of inhibitor necessary to cause the decrease of 50% in HNE activity and is determined by Eq. 3 (Cheng and Prusoff, 1973):

$$IC_{50} = K_i \times \left(1 + \frac{[S]}{K_m}\right) \quad (3)$$

The inhibitory activity of peptides MGWCTASVPPQCYG and MGWCTASVPPQCYG$(GA)_7$ against PPE, HNE and wound exudate were evaluated using synthetic and natural substrates. The results were compared with the activity of elastatinal inhibitor as control. IC_{50} values obtained for peptides MGWCTASVPPQCYG, MGWCTASVPPQCYG$(GA)_7$ and elastatinal, using synthetic substrates, are presented in Table 2 and are within the range of 11–19 μM. Once again peptide MGWCTASVPPQCYG$(GA)_7$ shows the lowest IC_{50} value which is the result of a higher inhibitory activity already demonstrated by the K_i values. The ability of peptides MGWCTASVPPQCYG and MGWCTASVPPQCYG$(GA)_7$ to inhibit the hydrolysis of insoluble elastin by HNE was also evaluated. Peptides MGWCTASVPPQCYG and MGWCTASVPPQCYG$(GA)_7$ present lower IC_{50} values in comparison with elastatinal under our assay conditions. Peptide MGWCTASVPPQCYG$(GA)_7$ presents higher inhibitory activity in the presence of a natural substrate.

3.4. Determination of peptides inhibitory activity after incorporation into silk fibroin films

The differences in inhibitory activity between peptide MGWCTASVPPQCYG and MGWCTASVPPQCYG$(GA)_7$ might be related with the GA tail introduced in the C-terminal of peptide MGWCTASVPPQCYG$(GA)_7$. To test this hypothesis, peptides were incorporated in fibroin films prepared as described in the experimental section and, the decrease in activity was monitored after 1 h of incubation of fibroin films, containing peptide MGWCTASVPPQCYG, MGWCTASVPPQCYG$(GA)_7$ and elastatinal, with HNE. Fibroin film without peptides was used as control. It can be seen from Fig. 5 that the activity loss obtained for peptide MGWCTASVPPQCYG and MGWCTASVPPQCYG$(GA)_7$ is similar. The GA tail has a high affinity towards fibroin thus, after incorporation and film crystallization, this tail is no longer available to interact with the enzyme. This result indicates that the GA tail plays an important role in the inhibition of HNE.

Table 2
Inhibitory activity of peptide and elastatinal against PPE, HNE and wound exudate using synthetic and natural substrates. (Peptide 2 = MGWCTASVPPQCYG, peptide 3 = MGWCTASVPPQCYG$(GA)_7$).

Enzyme	IC_{50} (μM)		
	Peptide 2	Peptide 3	Elastatinal
PPE	18.7 ± 0.06	16.0 ± 0.06	13.8 ± 0.06
HNE	19.2 ± 0.07	11.5 ± 0.06	12.2 ± 0.05
Exudate	16.0 ± 0.09	13.1 ± 0.06	14.3 ± 0.07
HNE (insoluble elastin)	29.3 ± 0.1	25.3 ± 0.1	37.6 ± 0.09
Exudate (insoluble elastin)	31.8 ± 0.04	26.9 ± 0.05	41.9 ± 0.04

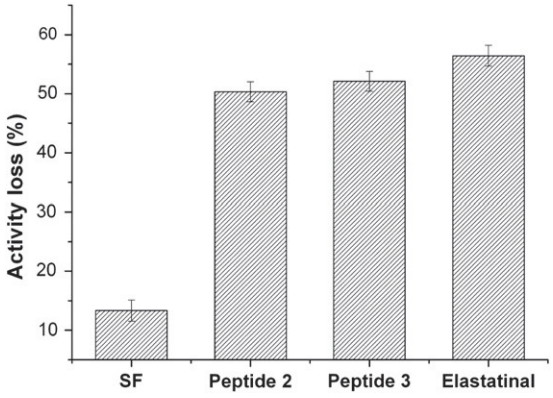

Fig. 5. Activity loss of HNE after 1 h of incubation at 25 °C with SF films incorporating peptide 2, 3 and elastatinal. (Peptide 2 = MGWCTASVPPQCYG, Peptide 3 = MGWCTASVPPQCYG$(GA)_7$).

3.5. Molecular-docking analysis

Molecular-docking analysis was done in order to better understand the mechanism of HNE inhibition by the new peptides. Docking calculations were made using AutoDock Vina version 1.1.1 (Trott and Olson, 2010). For the calculations we use the X-ray structure, PDB code 1B0F (Cregge et al., 1998), after removing the ligand present in this structure. This structure was used as the receptor without flexible side chains. The ligands were made flexible turning all possible bonds rotatable. Cyclic and amide bonds were considered as non-rotatable. Considering these we get 37 torsions for peptide 1, 44 torsions for peptide 2 and 72 torsions for peptide 3. For peptides 1 (WCTASVPPQCYG) and 2 (MGWCTASVPPQCYG) the grid size was chosen in order to included not only the known catalytic site of HNE but also the all the surrounding area. The surface in the opposite side of the enzyme was not considered. For the peptide 3 (MGWCTASVPPQCYG$(GA)_7$), and because this peptide is bigger, the grid was centered at the center of the protein and big enough to include all the protein and peptide 3 interacting with any spot of the surface. This procedure allows us to obtain the most favorable configuration representing the interaction between peptide 3 and HNE, without any kind of external impositions.

3.6. Cytotoxicity evaluation

The biocompatibility of the designed peptides was assessed through the use of fibroblast cultures. A preliminary screening was made using murine embryonic fibroblasts cells (MEFs) as a measure of global cytotoxicity. In this study, a wide range of peptide concentrations (from 20 to 80 μM) used for inhibition assays was evaluated and no toxicity was observed (Data not shown). The results obtained with MEFs were then confirmed with human skin fibroblasts, testing the lowest and highest peptide concentrations previously used and no additional damage to the cells was detected in any case. Fig. 7 shows the cell viability of human skin fibroblasts after 24 h (a) and 48 h (b) of incubation with the various peptides. In all cases, the cell viability was close to 100% indicating that peptides MGWCTASVPPQCYG and MGWCTASVPPQCYG$(GA)_7$ can be safely applied to the skin at these concentrations.

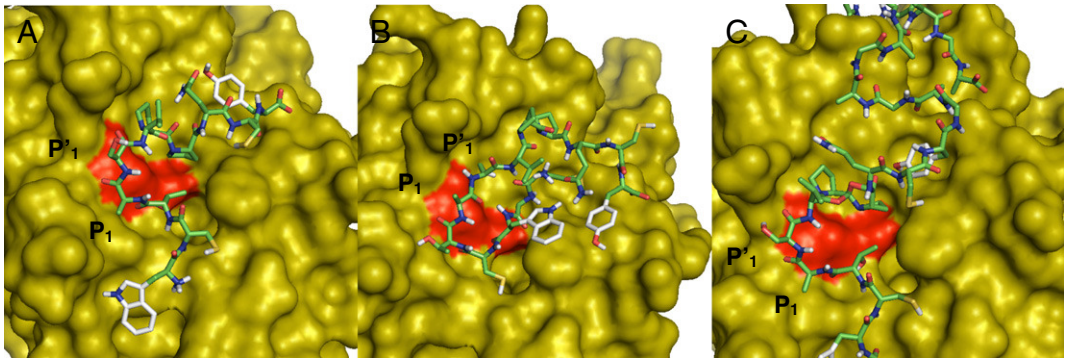

Fig. 6. Docking images of the interactions between HNE and peptides 1(A), 2(B) and 3(C). The catalytic triad is shown in red. (Peptide 2 = MGWCTASVPPQCYG, Peptide 3 = MGWCTASVPPQCYG$(GA)_7$).

4. Discussion

Accordingly to the nomenclature of Schechter and Berger (Schechter and Berger, 1967), the primary contact region between the inhibitor and the enzyme is the scissile peptide bond P1–P1′. Therefore, the specificity of the inhibition is dictated by the P1 residue which typically reflects the substrate preference of the target enzyme (Lu et al., 1997; Qasim et al., 1997). The peptide selected from the combinatorial library (Mcbride et al., 1999) has an alanine residue in the P1 position (Fig. 2). This residue in this position is consistent with the substrate specificity of elastase for small alkyl side chains (Harper et al., 1984; McRae et al., 1980; Stein et al., 1985). The stability and consequently the biological activity of the Bowman–Birk inhibitor-based peptides are supported by an extensive intramolecular hydrogen-bond network. The main-chain to main-chain hydrogen bond between P2 and P1′ (Fig. 2, dash lines) is responsible for projecting the P1 side-chain outwards for the primary interaction with the enzyme (Lin et al., 1993; Voss et al., 1996). The *cis*-Pro-*trans*-Pro motif in the P3′-P4′ positions and, the disulphide bridge covalently linking the P3–P6′ positions together with the hydrogen bond network guarantees the β-hairpin conformation typical of the Bowman–Birk inhibitor protein (Brauer et al., 2001; Mcbride et al., 1999; McBride et al., 2002). In this study, to this 9-residue motif, modifications were made in the N-terminal, by the introduction of methionine (M) and glycine (G) (Peptide 2, MGWCTASVPPQCYG, Fig. 2, light gray circles). This sequence was maintained and a glycine/alanine (GA) tail (n = 7) was added to the C-terminal (Peptide 3, MGWCTASVPPQCYG(GA)7, Fig. 2, dark gray circles).

The primary objective of adding this GA tail was to increase the affinity of this peptide to silk fibroin-based materials. In this way, fibroin-based wound dressings will be easily obtained with a specific biological activity: elastase inhibition (Vasconcelos et al., 2010). Nevertheless the results presented indicated that this GA tail has a very important role in the HNE inhibition. Peptide MGWCTASVPPQCYG$(GA)_7$, presented K_i and IC_{50} values for human elastase of 0.4 μM and 11.5 μM respectively. The K_i was 7-fold lower when compared with the peptide WCTASVPPQCYG (McBride et al., 2002) indicating a higher inhibitory activity. In contrast, the modifications introduced only at the N-terminal (peptide MGWCTASVPPQCYG) show a slightly improvement in the inhibition of PPE, but a worst result for the inhibition HNE when compared with peptide WCTASVPPQCYG. The better results obtained with peptide MGWCTASVPPQCYG$(GA)_7$ might be related to the increase in hydrophobicity resulting from the GA tail which corresponds to the preference of HNE for hydrophobic substrates. Although not possible, from the activity measurements, to quantify the exact number of binding sites, one might speculate that the potent binding between peptide MGWCTASVPPQCYG$(GA)_7$ and HNE might be due to the binding of this GA tail to the active center or adjacent active sites of HNE.

The amino acid composition of silk fibroin consists primarily of glycine, alanine and serine amino acids which form typical – (—ala-gly-)n – repeating motifs (Zhou et al., 2000). In the fiber, fibroin chains are aligned along the fiber axis held together by a close network of interchain hydrogen bonds with adjacent – (—ala-gly-)n – sequences forming the well known β-sheets crystals (Arai et al., 2001; Inoue et al., 2000). Therefore, peptide MGWCTASVPPQCYG$(GA)_7$ will

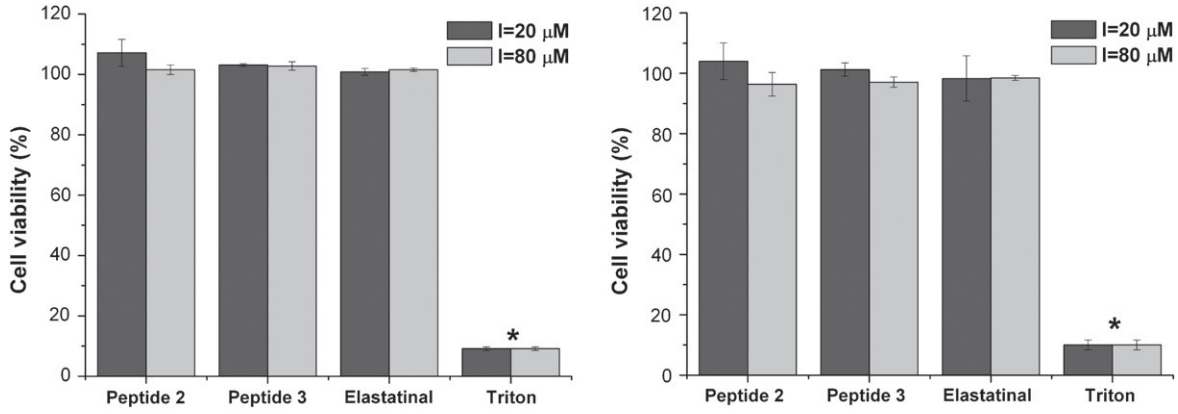

Fig. 7. Viability of human normal skin fibroblasts after 24 h (left panel) and 48 h (right panel) of contact with peptides 2, 3 and elastatinal. Only the positive control (treatment with Triton detergent) revealed diminished cell viability. (* = significantly different from all the other tested conditions, $P<0.05$). (Peptide 2 = MGWCTASVPPQCYG, Peptide 3 = MGWCTASVPPQCYG$(GA)_7$).

have a high affinity towards fibroin films due to the GA tail. The activity loss of HNE obtained in the presence of fibroin films incorporating peptides indicated that the inhibitory activity of peptide MGWCTASVPPQCYG$(GA)_7$ decreases. The activity loss obtained was similar to the one obtained for peptide 2 (MGWCTASVPPQCYG) which is a less potent inhibitor already demonstrated by inhibition kinetics results. This fact clearly demonstrates the importance of GA tail on the inhibitory activity. The loss in activity verified for peptide MGWCTASVPPQCYG$(GA)_7$ is explained by the fact that after film crystallization a transition from random coil to β-sheet of fibroin films occurs and the GA tail of this peptide may thus become a part of these β-sheet crystals being unavailable for the inhibitory activity.

Docking analysis indicated that the reactive site-loop of the Bowman–Birk inhibitor-peptides occupied most of the active site, inhibiting the HNE activity as already demonstrated by others (Mcbride et al., 1999; Nishino et al., 1977; Odani and Ikenaka, 1973; Terada et al., 1978). This also confirms the competitive inhibition obtained for Bowman–Birk inhibitor-peptides that was confirmed by our kinetic analysis. Nevertheless, modifications made on the C- and N-terminal of peptides had influence on the binding mode to the active site of HNE.

Peptide MGWCTASVPPQCYG had two more residues (MG) at the N-terminal, which increases the hydrophobic interactions between P and P′ side-chains (methionine is hydrophobic) thereby closing the loop (Fig. 6B) when compared to peptide WCTASVPPQCYG (Fig. 6A). This might increase the distance of P1 (Ala) to the active centre decreasing the inhibition. On the other hand, the increase in hydrophobicity of peptide MGWCTASVPPQCYG$(GA)_7$, given by the GA tail at the C-terminal causes the opening of the loop (Fig. 6C). This peptide showed the best HNE inhibitory activity. Docking analysis suggested that the primary interaction with the active site is also made by the P1, as observed for the other two peptides. Nevertheless the interaction of peptide MGWCTASVPPQCYG$(GA)_7$ with the enzyme tends to be more favorable. The hydrophobic GA tail has the ability to interact with the remaining enzyme, leading to a stronger interaction between the two species (Fig. 6C). This is consistent with what others observed for this particular enzyme. It was shown that HNE activity increases with the length of the synthetic substrates indicating that HNE has an extended binding site (Bode et al., 1986; Lestienne and Bieth, 1980). It is possible, as shown by docking analysis, that HNE accommodates the GA tail due to the high length and hydrophobicity leading to stronger interactions and, therefore, to higher inhibition rates.

Conclusion

The results presented in this study confirmed the ability of Bowman–Birk inhibitor peptides to inhibit human neutrophil elastase (HNE). Peptide MGWCTASVPPQCYG and MGWCTASVPPQCYG$(GA)_7$ are competitive inhibitors of HNE being peptide MGWCTASVPPQCYG $(GA)_7$ the one that presents higher inhibitory activity. This is due to the presence of the GA tail that increases hydrophobicity. Consequently, the affinity for HNE increases because of the preference of this enzyme for hydrophobic residues. The importance of the GA tail in the inhibition HNE was confirmed by incorporating peptides in a silk fibroin matrix and by molecular-docking analysis. After incorporation and subsequent crystallization of fibroin films, the inhibitory activity was similar to that obtained for peptide MGWCTASVPPQCYG. This happens because the GA tail, upon crystallization, is no longer available for the inhibition.

Peptide MGWCTASVPPQCYG and MGWCTASVPPQCYG$(GA)_7$ were also able to inhibit HNE present on a chronic wound exudate. This fact, along with the cytocompatibility observed with human skin fibroblasts, indicates that these peptides, especially peptide MGWCTASVPPQCYG$(GA)_7$, are potential bioactive agents against deleterious HNE-derived inflammatory episodes such as chronic wounds.

Acknowledgments

We would like to acknowledge FCT — Portuguese Foundation for Science and Technology for the scholarship concession; European project Lidwine, contract no. NMP2-CT-2006-026741.

References

Arai, T., Freddi, G., Colonna, G.M., Scotti, E., Boschi, A., Murakami, R., Tsukada, M., 2001. Absorption of metal cations by modified *B. mori* silk and preparation of fabrics with antimicrobial activity. J. Appl. Polym. Sci. 80, 297–303.

Bode, W., Wei, A.Z., Hber, R., Meyer, E., Travis, J., Neumann, S., 1986. X-ray crystal structure of the complex of human leukocyte elastase (PMN elastase) and the third domain of the turkey ovomucoid inhibitor. EMBO J. 5, 2453–2458.

Brauer, A.B.E., Kelly, G., McBride, J.D., Cooke, R.M., Matthews, S.J., Leatherbarrow, R.J., 2001. The Bowman–Birk inhibitor reactive site loop sequence represents an independent structural β-hairpin motif. J. Mol. Biol. 306, 799–807.

Chen, P., Rose, J., Love, R., Wei, C.H., Wang, B.C., 1992. Reactive sites of an anticarcinogenic Bowman–Birk proteinase inhibitor are similar to other trypsin inhibitors. J. Biol. Chem. 267, 1990–1994.

Cheng, Y., Prusoff, W.H., 1973. Relationship between the inhibition constant (K_I) and the concentration of inhibitor which causes 50 per cent inhibition (I50) of an enzymatic reaction. Biochem. Pharmacol. 22, 3099–3108.

Cregge, R.J., Durham, S.L., Farr, R.A., Gallion, S.L., Hare, C.M., Hoffman, R.V., Janusz, M.J., Kim, H.-O., Koehl, J.R., Mehdi, S., Metz, W.A., Peet, N.P., Pelton, J.T., Schreuder, H.A., Sunder, S., Tardif, C., 1998. Inhibition of human neutrophil elastase. 4. Design, synthesis, X-ray crystallographic analysis, and structural activity relationships for a series of P2-modified, orally active peptidyl pentafluoroethyl ketones. J. Med. Chem. 41, 2461–2480.

Domingo, G.J., Leatherbarrow, R.J., Freeman, N., Patel, S., Weir, M., 1995. Synthesis of a mixture of cyclic peptides based on the Bowman–Birk reactive site loop to screen for serine protease inhibitors. Int. J. Pept. Protein Res. 46, 79–87.

Edwards, P.D., Bernstein, P.R., 1994. Synthetic inhibitors of elastase. Med. Res. Rev. 14, 127–194.

Ekerot, L., Ohlsson, K., 1984. Interactions of granulocyte proteases with inhibitors in rheumatoid arthritis. Adv. Exp. Med. Biol. 167, 335–344.

Gariani, T., McBride, J.D., Leatherbarrow, R.J., 1999. The role of the P2′ position of Bowman-Birk proteinase inhibitor in the inhibition of trypsin: studies on P2′ variation in cyclic peptides encompassing the reactive site loop. BBA — Protein Struct. M. 1431, 232–237.

GraphPad, 2010. Software, I., v 5.03, USA.

Grinnell, F., Zhu, M., 1994. Identification of neutrophil elastase as the proteinase in burn wound fluid responsible for degradation of fibronectin. J. Invest. Dermatol. 103, 155–161.

Harper, J.W., Cook, R.R., Roberts, C.J., McLaughlin, B.H., Powers, J.C., 1984. Active site mapping of the serine proteases human leukocyte elastase, cathepsin G, porcine pancreatic elastase, rat mast cell proteases I and II, bovine chymotrypsin A, alpha, and *Staphylococcus aureus* protease V-8 using tripeptide thiobenzyl ester substrates. Biochemistry 23, 2995–3002.

Inoue, S., Tanaka, K., Arisaka, F., Kimura, S., Ohtomo, K., Mizuno, S., 2000. Silk fibroin of *Bombyx mori* is secreted, assembling a high molecular mass elementary unit consisting of H-chain, L-chain, and P25, with a 6:6:1 molar ratio. J. Biol. Chem. 275, 40517–40528.

Leatherbarrow, R.J., 1990. Using linear and non-linear regression to fit biochemical data. Trends Biochem. Sci. 15, 455–458.

Lestienne, P., Bieth, J.G., 1980. Activation of human leukocyte elastase activity by excess substrate, hydrophobic solvents, and ionic strength. J. Biol. Chem. 255, 9289–9294.

Lin, G., Bode, W., Huber, R., Chi, C., Engh, R.A., 1993. The 0.25-nm X-ray structure of the Bowman–Birk-type inhibitor from mung bean in ternary complex with porcine trypsin. Eur. J. Biochem. 212, 549–555.

Lowry, O.H., Rosebrough, N.J., Farr, A.L., Randall, R.J., 1951. Protein measurement with the folin phenol reagent. J. Biol. Chem. 193, 265–275.

Lu, W., Apostol, I., Qasim, M.A., Warne, N., Wynn, R., Zhang, W.L., Anderson, S., Chiang, Y.W., Ogin, E., Rothberg, I., Ryan, K., Laskowski, M., 1997. Binding of amino acid side-chains to S1 cavities of serine proteinases. J. Mol. Biol. 266, 441–461.

McBride, J.D., Leatherbarrow, R.J., 2001. Synthetic peptide mimics of the Bowman–Birk inhibitor protein. Curr. Med. Chem. 8, 909–917.

Mcbride, J.D., Freeman, H.N.M., Leatherbarrow, R.J., 1999. Selection of human elastase inhibitors from a conformationally constrained combinatorial peptide library. Eur. J. Biochem. 226, 403–412.

McBride, J.D., Watson, E.M., Brauer, A.B.E., Jaulent, A.M., Leatherbarrow, R.J., 2002. Peptide mimics of the Bowman–Birk inhibitor reactive site loop. Peptide Sci. 66, 79–92.

McRae, B., Nakajima, K., Travis, J., Powers, J.C., 1980. Studies on reactivity of human leukocyte elastase, cathepsin G, and porcine pancreatic elastase toward peptides including sequences related to the reactive site of .alpha.1-protease inhibitor (.alpha.1-antitrypsin). Biochemistry 19, 3973–3978.

Trott, O., Olson, A.J., 2010. AutoDock Vina: improving the speed and accuracy of docking with a new scoring function, efficient optimization, and multithreading. J. Comput. Chem. 31, 455–461.

Naughton, M.A., Sanger, F., 1961. Purification and specificity of pancreatic elastase. Biochem. J. 78, 156–163.
Nishino, N., Aoyagi, H., Kato, T., Izumiya, N., 1977. Studies on the synthesis of proteinase inhibitors. J. Biochem. 82, 901–909.
Norioka, S., Ikenaka, T., 1983. Amino acid sequences of trypsin-chymotrypsin inhibitors (A-I, A-II, B-I, and B-II) from peanut (*Arachis hypogaea*)1: a discussion on the molecular evolution of legume Bowman-Birk type inhibitors. J. Biochem. 94, 589–598.
Odani, S., Ikenaka, T., 1973. Scission of soybean Bowman-Birk proteinase inhibitor into two small fragments having either trypsin or chymotrypsin inhibitory activity. J. Biochem. 74, 857–860.
Qasim, M.A., Ganz, P.J., Saunders, C.W., Bateman, K.S., James, M.N.G., Laskowski, M., 1997. Interscaffolding additivity. Association of P1 variants of Eglin c and of turkey ovomucoid third domain with serine proteinases. Biochemistry 36, 1598–1607.
Schechter, I., Berger, A., 1967. On the size of the active site in proteases. I. Papain. Biochemical and Biophysical Research Communications 27, 157–162.
Shapiro, S.D., 2002. Proteinases in chronic obstructive pulmonary disease. Biochem. Soc. T. 30, 98–102.
Stein, R.L., Trainor, D.A., Wildonger, R.A., Denis, M.B., 1985. Chapter 24. Neutrophil Elastase. Ann Rep Med Chem. Academic Press, pp. 237–246.
Terada, S., Sato, K., Kato, T., Izumiya, N., 1978. Inhibitory properties of nonapeptide loop structures related to reactive sites of soybean Bowman–Birk inhibitor. FEBS Lett. 90, 89–92.
Vasconcelos, A., Pêgo, A.P., Henriques, L., Lamghari, M., Cavaco-Paulo, A., 2010. Protein matrices for improved wound healing: elastase inhibition by a synthetic peptide model. Biomacromolecules 11, 2213–2220.
Voss, R.-H., Ulrich, E., Lars-Oliver, E., Gabriele, W., Young-Mi, K., Peter, F., 1996. Crystal structure of the bifunctional soybean Bowman-Birk inhibitor at 0.28-nm resolution. Eur. J. Biochem. 242, 122–131.
Werner, M.H., Wemmer, D.E., 1992. Three-dimensional structure of soybean trypsin/chymotrypsin Bowman–Birk inhibitor in solution. Biochemistry 31, 999–1010.
Yager, D.R., Chen, S.M., Ward, S.I., Olutoye, O.O., Diegelmann, R.F., Kelman Cohen, I., 1997. Ability of chronic wound fluids to degrade peptide growth factors is associated with increased levels of elastase activity and diminished levels of proteinase inhibitors. Wound Repair Regen. 5, 23–32.
Zhou, C.-Z., Confalonieri, F., Medina, N., Zivanovic, Y., Esnault, C., Yang, T., Jacquet, M., Janin, J., Duguet, M., Perasso, R., Li, Z.-G., 2000. Fine organization of *Bombyx mori* fibroin heavy chain gene. Nucl. Acids Res. 28, 2413–2419.